Impact of Correlated Inputs on the Output of the Integrate-and-fire Model

Jianfeng Feng David Brown

Computational Neuroscience Laboratory, The Babraham Institute, Cambridge CB2 4AT, UK

Abstract

For the integrate-and-fire model with or without reversal potentials, we consider how correlated inputs affect the variability of cellular output. For both models the variability of efferent spike trains measured by coefficient of variation of the interspike interval (abbreviated to CV in the remainder of the paper) is a nondecreasing function of input correlation. When the correlation coefficient is greater than 0.09, the CV of the integrate-and-fire model without reversal potentials is always above 0.5, no matter how strong the inhibitory inputs. When the correlation coefficient is greater than 0.05, CV for the integrate-and-fire model with reversal potentials is always above 0.5, independent of the strength of the inhibitory inputs. Under a given condition on correlation coefficients we find that correlated Poisson processes can be decomposed into independent Poisson processes. We also develop a novel method to estimate the distribution density of the first passage time of the integrate-and-fire model.

1 Introduction

Although the single neurone model has been widely studied using computer simulation, most of these studies have made the assumption that inputs are independent (Brown & Feng, 1999; Feng, 1997; Feng & Brown, 1998a; Feng & Brown, 1998b; Tuckwell, 1988) both spatially and temporally. This assumption obviously contradicts the physiological data which clearly shows (1) that nearby neurones usually fire in a correlated way (Zohary et al., 1994) – what we term spatial correlation – and (2) neurones with similar functions frequently form groups and fire together. In fact 'firing together, coming together' is a basic principle in neuronal development (Sheth et al., 1996). Furthermore data in (Zohary et al., 1994) show that even a weak correlation within a population of neurones can have a substantial impact on network behaviour, which suggests that when comparing simulation results with experimental data, it is of vital importance to investigate the effects of correlated input signals on the output of single cells.

In this paper we address the following two important issues: how correlation between the inputs affects the output of single neurone models; when and how correlated inputs can be transformed into equivalent independent inputs. The second issue is interesting since it is usually not easy to model or analyse a correlated system, except

when it is Gaussian distributed. Theoretically we do not have general analytical tools to handle correlated systems, even to find analytical expressions for the distribution. It is even difficult numerically to generate a correlated random vector. Therefore a transformation from correlated to independent inputs greatly simplifies the problem, both theoretically and numerically, and furthermore provides insights on the functional role of the correlation. The technique can be applied to both simulation of biophysical models and to experiments, in order to generate correlated Poisson inputs.

The neuronal model used in this paper is the integrate-and-fire model with or without reversal potentials. Positive correlation in input signals usually enlarges the CV of the integrate-and-fire model. When the correlation coefficient is greater than 0.09 we find that CV for the leaky integrate-and-fire model *without* reversal potentials is always greater than 0.5. When the correlation coefficient is greater than 0.05, CV for the equivalent model *with* reversal potentials is always greater than 0.5. In recent years there has been much research devoted to finding a neuronal mechanism which can generate spike trains with a CV greater than 0.5 (see Brown & Feng, 1999; Feng, 1999; Feng & Brown, 1998b; Feng & Brown, 1999a; Konig et al., 1996) and references therein). To the best of our knowledge, this is the first paper to provide a possible mechanism for doing this for the integrate-and-fire model independently of the ratio between the inhibitory and excitatory inputs. Independently and experimentally, Stevens and Zador (1998) found that correlation between inputs was necessary in order to generate a sufficiently large CV in output spike trains of neurons in neocortical slices. Our analysis and simulations therefore provide a theoretical explanation of their findings.

We also show that it is only under a restrictive condition that dependent inputs can be decomposed into independent inputs. Finally we also propose a novel method of finding the distribution density of the first passage time of the integrate-and-fire model.

Correlation usually imposes a strong restriction on the system and has a very profound impact on its output, as previous noted in the literature (Gawne & Richmond, 1993; Zohary et al., 1994). Imagining a neurone exclusively receiving EPSPs from a population of p excitatory neurones with mutually positive correlation coefficient c, then the output CV of the perfect integrate-and-fire neurone (see section 3) is proportional to $[1+(p^2-p)c/p]/N_{th} = [1+(p-1)c]/N_{th}$, where N_{th} is the number of EPSPs required for the cell to fire. The first term $1/N_{th}$ is well known (Softky & Koch, 1993; Abbott et al., 1997) and is responsible for what is usually termed 'the Central Limit Theorem' effect. The important difference between the first and second terms is that the latter depends on p which is usually a large number. The appearance of this factor here and not in the first term is due to the fact that the correlation is a second order statistical quantity. Hence even when c is small, say 0.1, the quantity $(p-1)c$ can be substantially greater than the first term, approaching or exceeding N_{th}, thus resulting in a high CV.

This is the second of our series of papers aiming to elucidate how more realistic inputs, in contrast to conventional i.i.d Poisson inputs which have been intensively studied in the literature, affect the outputs of simple neuronal models. We aim to describe as completely as possible the full spectrum of the behaviour inherent in these

models, documenting more thoroughly their restrictions and potential. Feng and Brown (1998b) have considered the behaviour of the integrate-and-fire model subject to independent inputs with different distribution tails. In the near future we will report on more complicated biophysical models with realistic inputs as we develop here and in Feng and Brown (1998b).

2 Models

In this section we define the models used, and then discuss the effects of including reversal potentials on the dynamic behaviour of the leaky integrate-and-fire model, attempting to elucidate the essential difference this makes to its behaviour.

Suppose that a cell receives EPSPs at p excitatory synapses and IPSPs at q inhibitory synapses. The activities among excitatory synapses and inhibitory synapses are correlated but, for simplicity of notation here, we assume that the activities of the two classes are independent of each other. When the membrane potential V_t is between the resting potential V_{rest} and the threshold V_{thre},

$$dV_t = -\frac{1}{\gamma}V_t dt + a\sum_{i=1}^{p} dE_i(t) - b\sum_{j=1}^{q} dI_j(t) \tag{2.1}$$

where $1/\gamma$ is the decay rate, $E_i(t), I_i(t)$ are Poisson processes with rate λ_E and λ_I respectively and a, b are magnitude of each EPSP and IPSP (Thomson, 1997). Once V_t crosses V_{thre} from below a spike is generated and V_t is reset to V_{rest}. This model is termed the integrate-and-fire model. The interspike interval of the efferent spike process is

$$T = \inf\{t : V_t \geq V_{thre}\}$$

Without loss of generality we assume that the correlation coefficient between ith excitatory (inhibitory) synapse and jth excitatory (inhibitory) synapse is

$$c(i,j) = \frac{\langle (E_i(t) - \langle E_i(t)\rangle)(E_j(t) - \langle E_j(t)\rangle)\rangle}{\sqrt{\langle (E_i(t) - \langle E_i(t)\rangle)^2\rangle \cdot \langle (E_j(t) - \langle E_j(t)\rangle)^2\rangle}} = \rho(||i-j||)$$

where ρ is a non-increasing function. More specifically we consider two structures for the correlation: block-type correlation and Gaussian-type correlation. Here block-type correlation means that N cells are divided into N/k blocks and cell activities inside each block are correlated, whereas between blocks they are independent; Gaussian-type correlation implies that the correlation between cells is a decreasing function of their geometrical distance (we impose a periodic boundary condition).

A slightly more general model than the integrate-and-fire model defined above is the integrate-and-fire model with reversal potentials defined by

$$dZ_t = -\frac{Z_t - V_{re}}{\gamma}dt + \bar{a}(V_E - Z_t)\sum_{i=1}^{p} dE_i(t) + \bar{b}(V_I - Z_t)\sum_{j=1}^{q} dI_j(t) \tag{2.2}$$

where V_{re} is the resting potential, $\bar{a}, \bar{b}$ are the magnitude of single EPSP and IPSP respectively, V_E and V_I are the reversal potentials. Z_t (membrane potential) is now a birth-and-death process with boundaries V_E and V_I. Once Z_t is below V_{re} the decay term $Z_t - V_{re}$ will increase membrane potential Z_t; whereas when Z_t is above V_{re} the decay term will decrease it.

A detailed analysis might clarify the essential difference between the models with and without reversal potentials. Rewriting the model with reversal potentials Eq. (2.2) in the following way

$$\begin{aligned} dZ_t &= -\frac{Z_t - V_{re}}{\gamma}dt + \bar{a}(V_E - V_{re})\sum_{i=1}^{p} dE_i(t) + \bar{b}(V_I - V_{re})\sum_{j=1}^{q} dI_j(t) \\ &\quad -\bar{a}(Z_t - V_{re})\sum_{i=1}^{p} dE_i(t) - \bar{b}(Z_t - V_{re})\sum_{j=1}^{q} dI_j(t) \end{aligned} \tag{2.3}$$

We see that the term

$$-(Z_t - V_{re})/\gamma dt + \bar{a}(V_E - V_{re})\sum_{i=1}^{p} dE_i(t) + \bar{b}(V_I - V_{re})\sum_{j=1}^{q} dI_j(t)$$

is exactly the same as the integrate-and-fire model without reversal potentials, i.e. the coefficients of the diffusion term are fixed and independent of time. Compared to the integrate-and-fire model without reversal potentials, there is an additional term

$$-\bar{a}(Z_t - V_{re})\sum_{i=1}^{p} dE_i(t) - \bar{b}(Z_t - V_{re})\sum_{j=1}^{q} dI_j(t)$$

which is a pure decay term. Hence Eq. (2.3) can be expressed in the following way

$$\begin{aligned} dZ_t &= -(Z_t - V_{re})[\frac{1}{\gamma}dt + \bar{a}\sum_{i=1}^{p} dE_i(t) + \bar{b}\sum_{j=1}^{q} dI_j(t)] \\ &\quad +\bar{a}(V_E - V_{re})\sum_{i=1}^{p} dE_i(t) + \bar{b}(V_I - V_{re})\sum_{j=1}^{q} dI_j(t) \end{aligned} \tag{2.4}$$

Therefore, the model with reversal potentials essentially increases the decay rate of membrane potential, resulting in the system forgetting its dynamic history more quickly. This property is important when we consider how a group of cells synchronise their behaviour (Feng & Brown, 1999b), and is also important for understanding numerical differences in the behaviour of models with and without reversal potentials as presented below. Furthermore Eq. (2.4) might help us reach a theoretical conclusion on a debate (Tuckwell, 1988 at page 165; Wilbur & Rinzel, 1983) which has existed in the literature for decades.

3 Analytical Results

In this section, we first use the technique of martingale decomposition to approximate the input to the integrate-and-fire model. Together with the result in Appendix A, this

leads in Theorem 1 to a formula for the distribution of interspike interval for the *perfect* integrate-and-fire model subjected to correlated inputs. We then obtain (in Lemma 1) the interspike interval distribution of the *leaky* integrate-and-fire model for the special case when the leakage rate is such that the attractor of the deterministic part of the dynamics (Feng & Brown, 1999a) coincides with the spiking threshold. From this result, we find an expression in Theorem 2 for the distribution density of interspike interval for the general leaky integrate-and-fire model, which is then discussed. Finally the model with reversal potentials is considered.

First then, martingale decomposition is used to approximate the integrate-and-fire model with or without reversal potentials. We do not discuss the approximation accuracy since it has been done by many authors previously (Tuckwell, 1988; Ricciardi & Sato, 1990) (see section 5). The Poisson point processes representing EPSP and IPSP input involves perturbations of membrane potential with the following two properties. First, they are either fixed in size (for the model without reversal potentials) or of size dependent on membrane potential (for the model with reversal potentials). Secondly they arrive irregularly in time according to Poisson processes. Using martingale decomposition, we effectively rewrite this process as a Wiener or Brownian motion process, which is simulated as a sum of (1) an equivalent continuous current input representing the drift which occurs with unbalanced EPSP/IPSP input and (2) unbiased random input involving independently varying, small random perturbations of membrane potential, arriving at regularly spaced, very short intervals of time.

The martingale decomposition reads

$$E_i(t) \sim \lambda_E t + \sqrt{\lambda_E} B_i^E(t)$$

and similarly

$$I_i(t) \sim \lambda_I t + \sqrt{\lambda_I} B_i^I(t)$$

where $B_i^E(t)$ and $B_i^I(t)$ are standard Brownian motions. For fixed time t the above decomposition is equivalent to the central limit theorem. Therefore the integrate-and-fire model without reversal potentials can be approximated by

$$dv_t = -\frac{1}{\gamma} v_t dt + a\sum_{i=1}^{p} \lambda_E dt - b\sum_{i=1}^{q} \lambda_I dt + a\sqrt{\lambda_E}\sum_{i=1}^{p} dB_i^E(t) - b\sqrt{\lambda_I}\sum_{i=1}^{q} dB_i^I(t)$$

Since the summation of Brownian motions is again a Brownian motion we can rewrite the equation above as follows

$$\begin{aligned} dv_t &= -\frac{1}{\gamma} v_t dt + (ap\lambda_E - bq\lambda_I)dt \\ &\quad + \sqrt{a^2\lambda_E \sum_{i=1}^{p}\sum_{j=1}^{p} c^E(i,j) + b^2\lambda_I \sum_{i=1}^{q}\sum_{j=1}^{q} c^I(i,j)}\, dB(t) \\ &= -\frac{1}{\gamma} v_t dt + (ap\lambda_E - bq\lambda_I)dt \\ &\quad + \sqrt{a^2 p\lambda_E + b^2 q\lambda_I + a^2\lambda_E \sum_{i\neq j}^{p} c^E(i,j) + b^2\lambda_I \sum_{i\neq j}^{q} c^I(i,j)}\, dB(t) \end{aligned} \tag{3.1}$$

When $c^E(i,j) = c^I(i,j) = 0$ Eq. (3.1) gives rise to the same results as in the literature (Tuckwell, 1988) for independent inputs.

When $q = 0$ and $c^E(i,j) = c$, the signal-to-noise ratio given by Eq. (3.1) is

$$SNR = \frac{p\lambda_E}{\sqrt{p\lambda_E + p(p-1)\lambda_E c}}$$

which coincides with that in Zohary et al. (1994), Fig. 3 a).

Combining the results above with the conclusions in Appendix A we arrive at the following theorem for the perfect integrate-and-fire model. Let T be the first passage time of v_t.

Theorem 1 *If $\gamma = \infty$ the distribution density of T is*

$$\begin{aligned} p(t) &= \frac{V_{thre}}{\sqrt{2\pi(a^2 p\lambda_E + b^2 q\lambda_I + a^2\lambda_E \sum_{i\neq j}^{p} c^E(i,j) + b^2\lambda_I \sum_{i\neq j}^{q} c^I(i,j))t^3}} \\ &\quad \exp\left[-\frac{(V_{thre} - (ap\lambda_E - bq\lambda_I)t)^2}{2(a^2 p\lambda_E + b^2 q\lambda_I + a^2\lambda_E \sum_{i\neq j}^{p} c^E(i,j) + b^2\lambda_I \sum_{i\neq j}^{q} c^I(i,j))t}\right] \end{aligned} \tag{3.2}$$

and in particular

$$\begin{cases} \langle T\rangle &= \dfrac{V_{thre}}{ap\lambda_E - bq\lambda_I} \\ CV &= \dfrac{a^2 p\lambda_E + b^2 q\lambda_I}{V_{thre}(ap\lambda_E - bq\lambda_I)} + \dfrac{a^2\lambda_E \sum_{i\neq j}^{p} c^E(i,j) + b^2\lambda_I \sum_{i\neq j}^{q} c^I(i,j)}{V_{thre}(ap\lambda_E - bq\lambda_I)} \end{cases} \tag{3.3}$$

Theorem 1 tells us that, for the perfect integrate-and-fire model, correlation between inputs does impact on the variation of output interspike interval, but not on the mean firing rate. Compared to the perfect integrate-and-fire model without correlation, the CV of efferent interspike intervals falls between 0.5 and 1 for greater degrees of imbalance between EPSPs and IPSPs (Feng & Brown, 1998b). Furthermore the output distribution is a long-tailed distribution if and only if an exact balance between EPSPs and IPSPs is reached, although in general correlated inputs will generate efferent spikes with a larger CV. Although Theorem 1 is a special case of Theorem 2, we prefer to write it as a separate theorem since we apply it in the next section.

In Appendix A, we present a new and simple proof of Theorem 1 without resorting to the classic Laplace transformation (Tuckwell, 1988) which, we hope, opens up new possibilities for obtaining an analytical formula for general cases–the integrate-and-fire model without reversal potentials. The idea of our approach is to use Girsanov's Theorem (Protter, 1980), which connects two diffusion processes with a displacement transformation. Once we know the properties of the following diffusion process ($\sigma > 0$, a constant)

$$dX_t = b(X_t)dt + \sigma dB_t$$

we can, by Girsanov's Theorem, infer properties of the following diffusion process

$$dY_t = b(Y_t)dt + \mu dt + \sigma dB_t$$

For the problem we consider here we can find the distribution density of the following case

$$d\bar{v}_t = -\bar{v}_t/\gamma dt + \mu_0 dt + \sigma dB_t$$

with

$$\mu_0 = V_{thre}/\gamma, \tag{3.4}$$

i.e. the special case that the attractor of the deterministic dynamics coincides with the threshold. For further interesting properties of the dynamics under the condition Eq. (3.4), we refer the reader to (Feng, 1999; Feng & Brown, 1999a). Let $\bar{T}$ be the first passage time of $\bar{v}_t$.

Lemma 1 *When $\mu = V_{thre}/\gamma$ the distribution density of $\bar{T}$ is given by*

$$p_0(t) = \frac{2\sigma^2 V_{thre}\exp(-t/\gamma)}{\sqrt{\pi[\sigma^2\gamma(1-\exp(-2t/\gamma))]^3}} \cdot \exp[-\frac{V_{thre}^2\exp(-2t/\gamma)}{\sigma^2\gamma(1-\exp(-2t/\gamma))}] \tag{3.5}$$

Hence, by using Girsanov's Theorem, as we do in the Appendix, we find an analytical formula for the general case

$$dv_t = -v_t/\gamma dt + \mu_0 dt + (\mu-\mu_0)dt + \sigma dB_t$$

as described below.

Theorem 2 *The distribution density of the first passage time T of v_t is*

$$\begin{aligned} p(t) &= p_0(t)\exp[-(\frac{(\mu-\mu_0)^2 t}{2\sigma^2} + \frac{V_{thre}(\mu-\mu_0)}{\sigma^2}]\exp(\frac{-(\mu-\mu_0)\mu_0 t}{\sigma^2}) \\ &\quad \langle\exp(\frac{\mu-\mu_0}{\sigma^2}\cdot\int_0^{\bar{T}}\frac{\bar{V}_t}{\gamma})dt|\mathcal{F}_{\bar{T}}\rangle_{\bar{T}=t} \end{aligned} \tag{3.6}$$

As in the appendix we only need to calculate the Radon-Nikodyn derivative in Girsanov's Theorem which is given by

$$\begin{aligned} F(t) &= \exp(\int_0^t \frac{1}{\sigma}(\mu-\mu_0)dB_s - \frac{1}{2}\int_0^t \frac{(\mu-\mu_0)^2}{\sigma^2}ds) \\ &= \exp(\frac{\mu-\mu_0}{\sigma}B_t - \frac{1}{2}\frac{(\mu-\mu_0)^2}{\sigma^2}t) \end{aligned}$$

Therefore we have

$$\langle g(T)\rangle = \int_0^\infty g(t)p_0(t)\exp(-\frac{(\mu-\mu_0)^2}{2\sigma^2}t)\langle\exp(\frac{\mu-\mu_0}{\sigma}B_{\bar{T}}|\mathcal{F}_{\bar{T}})\rangle_{\bar{T}=t}\,dt \tag{3.7}$$

where g is a measurable, non-negative function and T is the first passage time, $\mathcal{F}_t$ is the σ-algebra up to time t. Now the only remaining task to prove Theorem 2 is to find an analytical formula for $B_{\bar{T}}$. From

$$d\bar{v}_t = -\bar{v}_t/\gamma dt + \mu_0 dt + \sigma dB_t$$

we have

$$\bar{v}_{\bar{T}} = -\int_0^{\bar{T}} \bar{v}_t dt/\gamma + \mu_0 \bar{T} + \sigma B_{\bar{T}}$$

Eq. (3.7) thus becomes

$$\begin{aligned}\langle g(T)\rangle &= \int_0^{\infty} g(t)p_0(t)\exp[-(\frac{(\mu-\mu_0)^2 t}{2\sigma^2} + \frac{V_{thre}(\mu-\mu_0)}{\sigma^2}]\exp(\frac{-(\mu-\mu_0)\mu_0 t}{\sigma^2}) \\ &\quad \langle \exp(\frac{\mu-\mu_0}{\sigma^2}\cdot\int_0^{\bar{T}}\frac{\bar{v}_t}{\gamma}dt)|\mathcal{F}_{\bar{T}}\rangle_{\bar{T}=t}\, dt\end{aligned}$$

which gives the desired results.

Now let us consider the meaning of the term $\int_0^{\bar{T}} \bar{v}_t dt$. It is the area under the curve visited by the process $\bar{v}_t$, before it hits the threshold as shown in Fig. 1. It is easily seen that we are able to use different ways to approximate $\int_0^{\bar{T}} \bar{v}_t dt$ (we know the distribution of $\bar{T}$, Lemma 1) which gives rise to various approximations of the distribution density of T.

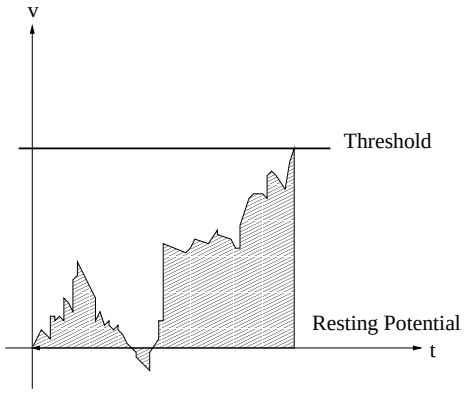

Figure 1: Dark area above the resting potential $-$ Dark area below the resting potential=$\int_0^{\bar{T}} \bar{v}_t dt$ ($V_{rest} = 0mV$).

To find an analytical formula for the distribution density of T is a problem studied for decades, and a number of different methods, mainly in terms of PDEs, have been employed (see for example Ricciardi & Sato, 1990). Here we present a novel and probably the most natural way – by virtue of the probability method – to approximate the distribution density. A study on how to improve the accuracy of the approximation is an interesting problem, but it is outside the scope of the present paper and will be published elsewhere.

In fact, from Theorem 2 we can obtain some informative conclusions. For example we claim that as soon as $\mu \geq \mu_0$, then $p(t)$ goes to zero ($t \to \infty$) faster than or equal to

$$\exp(-[\frac{(\mu-\mu_0)^2}{2\sigma^2} + \frac{1}{\gamma}]t)$$

an exponential decreasing function. This is because

$$\bar{v}_t/\gamma \leq V_{thre}/\gamma = \mu_0$$

and therefore

$$\exp(\frac{-(\mu-\mu_0)\mu_0 t}{\sigma^2})\langle\exp(\frac{\mu-\mu_0}{\sigma^2}\cdot\int_0^{\bar{T}}\frac{\bar{v}_t}{\gamma}dt)|\mathcal{F}_{\bar{T}}\rangle_{\bar{T}=t}\leq 1$$

Now we turn our attention to the model with reversal potentials. Similar to the above treatment of the model without reversal potentials, we can rewrite the model in the following form

$$\begin{aligned} dz_t &= -\frac{1}{\gamma}z_t dt + a\sum_{i=1}^{p}\lambda_E(V_E-z_t)dt + b\sum_{i=1}^{q}\lambda_I(V_I-z_t)dt \\ &\quad +a\sqrt{\lambda_E}\sum_{i=1}^{p}|V_E-z_t|dB_i^E(t) + b\sqrt{\lambda_I}\sum_{i=1}^{q}|V_I-z_t|dB_i^I(t) \end{aligned}$$

which gives

$$dz_t = -\frac{1}{\gamma}z_t dt + (ap(V_E-z_t)\lambda_E - bq(z_t-V_I)\lambda_I)dt + \sigma_r(t)dB_t \tag{3.8}$$

where

$$\begin{aligned} \sigma_r^2(t) &= a^2(z_t-V_E)^2\lambda_E\sum_{i=1}^{p}\sum_{j=1}^{p}c^E(i,j) \\ &\quad +b^2(z_t-V_I)^2\lambda_I\sum_{i=1}^{q}\sum_{j=1}^{q}c^I(i,j) \\ &= a^2(z_t-V_e)^2 p\lambda_E + b^2(z_t-V_I)^2 q\lambda_I + a^2(z_t-V_E)^2\lambda_E\sum_{i\neq j}^{p}c^E(i,j) \\ &\quad +b^2(z_t-V_I)^2\lambda_I\sum_{i\neq j}^{q}c^I(i,j) \end{aligned} \tag{3.9}$$

There are other forms for the diffusion terms in Eq. (3.8) to approximate the original process (Musila & Lansky, 1994). For simplicity of notation we confine ourselves to Eq. (3.9).

4 Numerical Results

From now on we assume that $c^E(i,j) = c^I(i,j) = c(i,j)$. In this section we present and discuss the results of numerical simulations showing the effect of block-type correlation on mean(ISI) and CV of the leaky integrate-and-fire model without (Fig. 2) and with reversal potentials (Fig. 4) for moderate EPSP/IPSP sizes, and also for very small EPSP/IPSP sizes (Fig. 3). We also demonstrate the effect of a correlation which falls off as an inverse square law (Fig. 5).

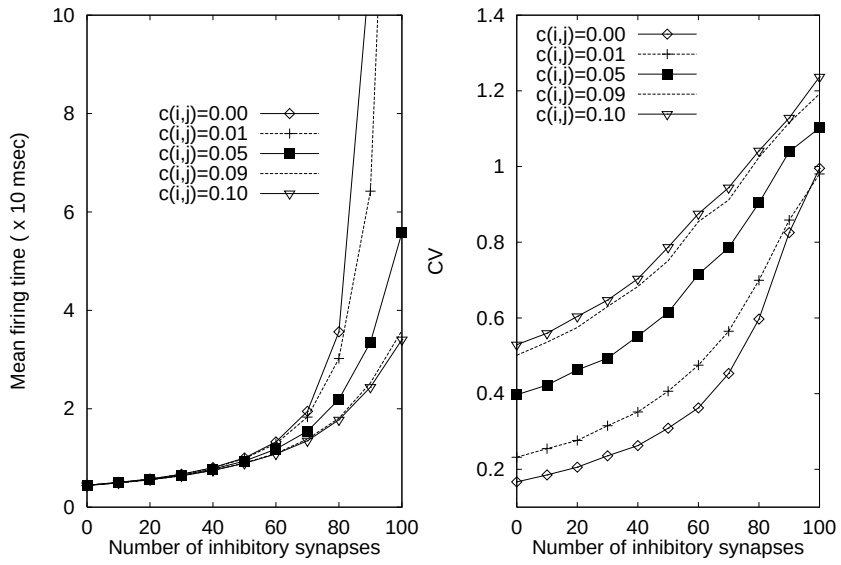

Figure 2: Mean firing time (left) and CV (right) vs. q for $c(i,j) = 0., 0.01, 0.05, 0.09, 0.1$ of the integrate-and-fire model without reversal potentials. 10000 spikes are generated for calculating the mean firing time and CV. Parameters are specified in the context. As soon as $c(i,j) \geq 0.09$ we see that CV of efferent spike trains is greater than 0.5.

4.1 Block-type Correlation

For simplicity of notation we only consider the case that $c(i,j) = c$ for $i \neq j, i, j = 1, \cdots, p$ and $i \neq j, i, j = 1, \cdots, q$. It is reported in the literature (Zohary et al., 1994) that the correlation coefficient between cells is around 0.1 in V5 of rhesus monkeys *in vivo*. In human motor units of a variety of muscles the correlation coefficients are usually in the range 0.1 to 0.3 (Matthews, 1996). In Fig. 2 we show numerical simulations for $q = 0, 10, 20, \cdots, 100, p = 100, V_{rest} = 0., V_{thre} = 20mV, a = b = 0.5mV, \gamma = 20.2msec$, a set of parameters as in the literature (Brown & Feng, 1999; Feng, 1999; Feng & Brown, 1998b, Feng & Brown, 1999a), and $c = 0, 0.01, 0.02, \cdots, 0.1$. When $c = 0$, inputs without correlation, there are many numerical and theoretical investigations (see for example Softky & Koch, 1993; Ricciardi & Sato, 1990; Feng & Brown, 1998b). As one might expect, the larger the input correlation, the larger the output CV. In particular we note that when $c \geq 0.09$, then $CV > 0.5$ for any value of q.

It is interesting to note that when the ratio q/p is small, the mean firing time is independent of the correlation, a phenomenon we have pointed out for the perfect integrate-and-fire model (Theorem 1). However when q/p is large (i.e. $q \geq 50$), the mean firing time with weak correlation is greater than that with large correlation. It can be easily understood from the properties of the process since the larger the correlation, the larger the diffusion term which will drive the process to cross the threshold more often. However, as in the perfect integrate-and-fire model, CV of efferent spike trains

does depend on the ratio and the correlation. The larger the correlation and the ratio, the larger the CV.

In recent years there have been many studies devoted to the problem of how to generate spike trains with CV between 0.5 and 1 (see for example Brown & Feng, 1999; Feng, 1999; Feng & Brown, 1998b; Feng & Brown, 1999a; Softky & Koch, 1993; Shadlen & Newsome, 1994). In particular it is pointed out in Softky & Koch (1993) that it is impossible for the integrate-and-fire model to generate spike trains with CV between 0.5 and 1 if the inputs are exclusively excitatory. A phenomenon referred to as 'central limit effect' is widely cited in the literature (Abbott et al., 1997), as justification of this statement. Many different approaches have been proposed to get around this problem (Shadlen & Newsome, 1994) In the present paper we clearly demonstrate that even with exclusively excitatory inputs the integrate-and-fire model is capable of emitting spike trains with CV greater than 0.5. No matter what the ratio between the excitatory and inhibitory synapses, the CV of efferent spike trains is always greater than 0.5, provided that the correlation coefficient between the inputs if greater or equal to 0.09. Furthermore we want to emphasize that in Zohary et al. (1994) the authors claim, based on their physiological data, that $c > 0.1$ is the most plausible case.

For further confirming that a small correlation plays an important role in neuronal output, in Fig. 3 we simulate an extreme case with EPSP and IPSP size of $0.05mV$. It has been reported (Shadlen & Newsome, 1994) that the size of EPSP is between 0.05 mV and 2mV. This choice implies that 400 EPSPs are needed to drive a cell to fire. To have a reasonable comparison with the numerical results of $a = 0.5$, μ is kept as a constant when the ratio q/p is the same and hence $p = 1000$ in Fig. 3. When $c(i,j) = 0$ and $q = 0$ CV is about 0.05 (see Fig. 3). Fig. 3 clearly shows that a large efferent CV is again obtained with a small correlation.

Now we turn to the integrate-and-fire model with reversal potentials. As we already pointed out above, the essential difference between this model and that without reversal potentials is that the latter has a large membrane potential decay rate. Therefore in this case it is natural to expect that a larger efferent spike train CV is obtained since the decay term plays a predominant role.

We assume that $V_{re} = -50mV, V_I = -60mV, V_{th} = -30$ and $V_E = 50mV$, values which match experimental data. As in the literature (Musila & Lansky, 1994; Feng & Brown, 1998b) we impose a local balance condition on the magnitude of EPSPs and IPSPs: $\bar{a}(V_E - V_{re}) = \bar{b}(V_{re} - V_I) = 1mV$ i.e. starting from the resting potential a single EPSP or a single IPSP will depolarize or hyperpolarize the membrane potential by 1mV (see the discussion in Section 3).

Figure 4 clearly shows that, as we mentioned above, efferent spike trains of the integrate-and-fire model with reversal potentials are more variable than for the model without reversal potentials (except for high q and $c(i,j)$). When the correlation coefficient is greater than 0.05, $CV > 0.5$, no matter what the ratio between inhibitory and excitatory inputs. Due to this effect (large CV) we see that mean firing rates are also more spread than for the model without reversal potentials. When $q \geq 20$ the difference between mean firing times become discernible (see Fig. 4).

From Fig. 2 and Fig. 4 we can see another interesting phenomenon. When q/p

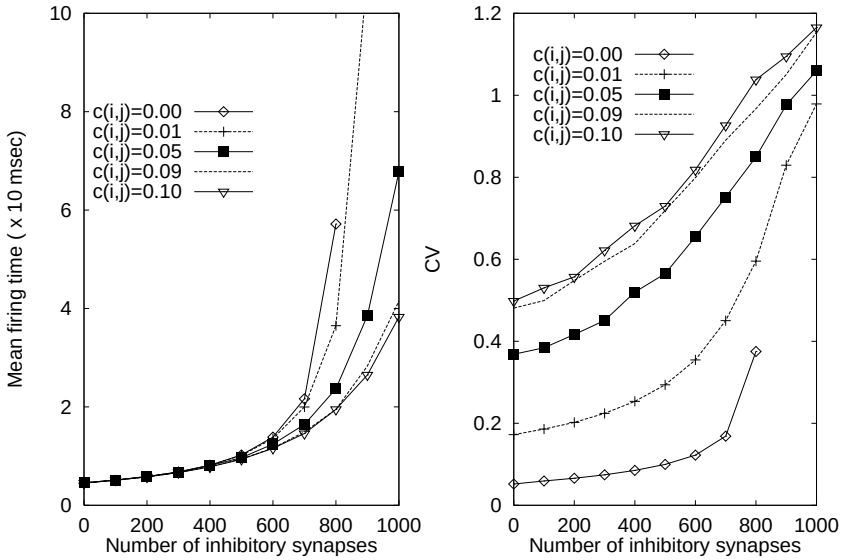

Figure 3: Mean firing time (left)and CV (right) vs. q for $c(i,j) = 0., 0.01, 0.05, 0.09, 0.1$ of the integrate-and-fire model without reversal potentials and $a = b = 0.05$, $p = 1000$. 10000 spikes are generated for calculating the mean firing time and CV. Parameters are specified in the context. For the case of $c(i,j) = 0$ and $q = 0$, CV is 0.05. Note that we only calculate $q = 0, 100, \cdots, 800$ for $c(i,j) = 0$ since the mean firing time is too large when $q = 900, 1000$.

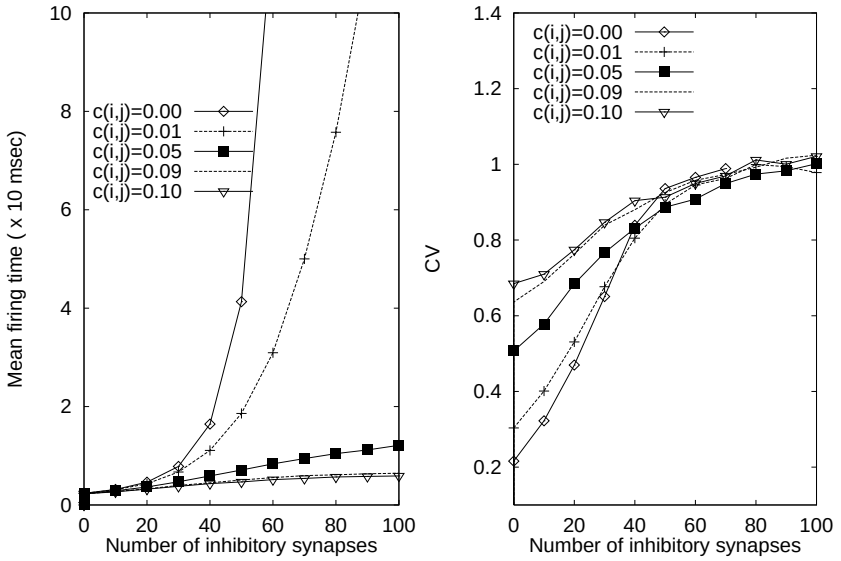

Figure 4: Mean firing time (left)and CV (right) vs. q for $c(i,j) = 0., 0.01, 0.05, 0.09, 0.1$ of the integrate-and-fire model with reversal potentials. 10000 spikes are generated for calculating the mean firing time and CV. Parameters are specified in the context. As soon as $c(i,j) \geq 0.05$ we see that CV of efferent spike trains is greater than 0.5.

approaches one, the CV of the integrate-and-fire model without reversal potential is greater than that of the model with reversal potentials (which itself is less than or equal to one) (see Tuckwell (1988) at page 165, Wilbur & Rinzel (1983)). The reason can be understood from our analyses in Section 3. Note that the decay term will return the system to the resting potential. The model with reversal potentials is equivalent to one with a large decay rate and so Z_t generally remains closer to the resting potential than V_t. When q gets close to 100 the deterministic forces tending to increase membrane potential become weak and so the process starting from the resting potential will tend to fall below the resting potential more and more often. However the decay terms together with the reversal potentials in the integrate-and-fire model with reversal potentials will prevent the process going far below the resting potential. The process Z_t is thus more densely packed in a compact region and a smaller range of CV is thus observed.

4.2 Gaussian-Type Correlation

We suppose that $c(i,j) = \exp(-(i-j)^2/\sigma^2), i,j = 1,\cdots,p$ with periodic boundary conditions. Hence the larger that σ is, the more widely spread the correlation for the ith cell. We simulate the integrate-and-fire model using the Euler scheme (Feng et al. 1992) with $\sigma = 1,2,\cdots,10$. Similar phenomena as in the previous subsection are observed (Fig.5): there is a threshold value σ_c, such that as soon as

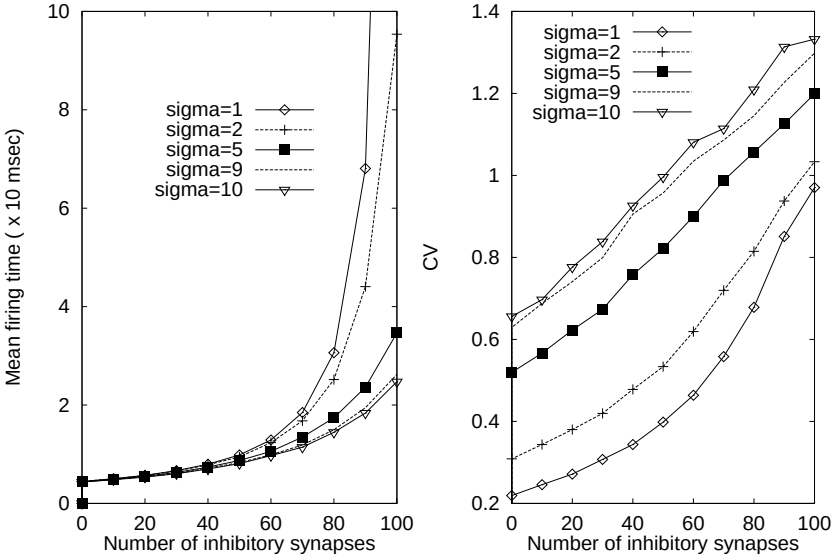

Figure 5: Mean firing time (left) and CV (right) vs. q for $\sigma = 1,2,5,9,10$ of the integrate-and-fire model without reversal potentials for a Gaussian-type correlation pattern. 10000 spikes are generated for calculating the mean firing time and CV. Parameters are specified in the context. As soon as $\sigma \geq 5$ we see that CV of efferent spike trains is greater than 0.5.

$\sigma > \sigma_c$, CV of efferent trains becomes greater than 0.5, independent of the number

of inhibitory inputs. Similar results are obtained for the integrate-and-fire model with reversal potentials (see the previous subsection) as well (not shown).

5 From Dependent To Independent Synapses

We now consider how we can realise a constant correlated Poisson process. Define $E_i(t) = N_i(t) + N(t)$ where $N_i(t), i = 1, \cdots, p$ are i.i.d. Poisson processes with rate $(1-c)\lambda_E$ and $N(t)$ is an independent Poisson process with rate $c\lambda_E$. It is then easily seen that the correlation coefficient between E_i and E_j is c. Therefore in terms of our conclusions above we can rewrite the total synaptic inputs $\sum_i E_i(t)$ in the following way

$$\sum_i E_i(t) = \sum N_i(t) + pN(t) \tag{5.1}$$

This conclusion tells us that constant correlated Poisson inputs are equivalent to the case where there is a common source, i.e. the term $N(t)$ in Eq. (5.1), for all synapses.

We usually prefer independent inputs - which are much easier to deal with than correlated inputs - and we do so again here. Let us rewrite the integrate-and-fire model in the following way.

$$\begin{aligned} dV_t &= -\frac{V_t}{\gamma}dt + a\sum_{i=1}^{p} dN_i^E(t) + apdN^E(t) - b\sum_{i=1}^{q} dN_i^I(t) - bqdN^I(t) \\ &\sim -\frac{V_t}{\gamma}dt + \mu dt \\ &\quad + \sqrt{a^2p(1-c)\lambda_E + b^2q(1-c)\lambda_I + a^2p^2c\lambda_E + b^2q^2c\lambda_E}\,dB_t \end{aligned}$$

We note that the independent term contributes to the variance term with an amount of $a^2p\lambda_E(1-c)$ but the common source contributes with an amount of $a^2p^2\lambda_E c$. Since usually p is large and thus the common source plays a predominant role in the model behaviour when we employ physiological parameters, i.e. $a = 0.5, c = 0.1$ in the integrate-and-fire model.

We thus ask ourselves whether a given series of correlated Poisson processes (suppose that $c(i,j), j = 1, \cdots, p$ is not a constant) can be decomposed into a series of independent Poisson processes. Furthermore, without loss of generality, we assume that $\lambda_E = 1$.

Theorem 3 *(Decomposition Theorem) Suppose that p is large and*

$$\sum_{j=2}^{p} c(1,j) \leq \frac{1}{2} \tag{5.2}$$

the Poisson process $E_i(t)$ defined below

$$E_i(t) = N_i(t) + \sum_{j=1}^{i-1} N_{j,i-j}(t) + \sum_{j=1}^{p-i} N_{i,j}(t)$$

is correlated with a correlation between $E_i(t)$ *and* $E_j(t)$ *equal to* $c(1,|i-j|), i \neq j, j \pm 1$, *where* $N_i(t), N_{i,j}(t), i = 1, \cdots, p; \quad j = 1, \cdots, p-i$ *are independent Poisson processes with rate* $\lambda_{N_i} = t(1 - \sum_{j=2}^{i-1} c(1,j) - \sum_{j=2}^{p-i} c(1,j))$ *and* $\lambda_{N_{i,j}} = tc(1,j)$.

Proof For $i \neq j, j+1, j-1$, we obtain

$$
\begin{aligned}
&< E_i(t) - < E_i(t) >, E_j(t) - < E_j(t) >> \\
&= < N_i(t) - < N_i(t) >, N_j(t) - < N_j(t) >> \\
&\quad + \sum_{k=1}^{i-1} \sum_{l=1}^{j-1} < N_{k,i-k}(t) - < N_{k,i-k}(t) >, N_{l,j-l}(t) - < N_{l,j-l}(t) >> \\
&\quad + \sum_{k=1}^{i-1} \sum_{l=1}^{p-j} < N_{k,i-k}(t) - < N_{k,i-k}(t) >, N_{j,l}(t) - < N_{j,l}(t) >> \\
&\quad + \sum_{k=1}^{p-i} \sum_{l=1}^{j-1} < N_{i,k}(t) - < N_{i,k}(t) >, N_{l,j-l}(t) - < N_{l,j-l}(t) >> \\
&\quad + \sum_{k=1}^{p-i} \sum_{l=1}^{p-j} < N_{i,k}(t) - < N_{i,k}(t) >, N_{j,l}(t) - < N_{j,l}(t) >> \\
&= \frac{1}{2}(1 + sgn(i-j))c(1,|i-j|)t + \frac{1}{2}(1 + sgn(j-i))c(1,|i-j|)t \\
&= c(1,|i-j|)t.
\end{aligned}
$$

Using a similar algebraic calculation, we have $< E_i(t) - < E_i(t) >, E_i(t) - < E_i(t) >>= t$ Therefore the correlation coefficient between $E_i(t)$ and $E_j(t)$ is given by $c(1,|i-j|)$.

It is obviously seen that condition (5.2) is rather restrictive since $c(i,j) = c$ with $c > 1/p$ violates it. However we have the following example which shows that the condition in Theorem 3 is a necessary and sufficient condition for a linear decomposition.

Example 1 Consider four cells $i = 1, 2, 3, 4$ and assume that $c(2,3) > 0$ and $c(2,4) = 0$. Since we have $c(1,3) = 0$ the most efficient way to construct E_2 is

$$E_2(t) = N_1(t) + N_3(t)$$

with $\langle N_1(t) \rangle = c(2,3) = \langle N_3(t) \rangle$. Therefore if and only if

$$2c(1,2) \leq 1$$

do we have a linear decomposition of $E_i(t)$.

6 Discussion

In this paper we have shown that a weak correlation between neurones can have a dramatic influence on model output. In the integrate-and-fire model without reversal potentials, when the correlation coefficient is above 0.09 the CV of efferent spike

trains is above 0.5. In the integrate-and-fire model with reversal potentials, when the correlation coefficient is above 0.05 the CV of efferent spike trains is greater than 0.5 already. The above properties are independent of the numbers of inhibitory inputs and therefore resolve an existing problem in the literature: how the integrate-and-fire model generates spike trains with CV greater than 0.5 when there is a low ratio between inhibitory and excitatory inputs. Note that Zohary et al. (1994) have claimed that a correlation greater than 0.1 is the most plausible value.

The integrate-and-fire model is one of the most widely used single neuronal models. The advantage when studying it is that there are some useful analytical formulas, although there is a fundamental question open: to find the distribution density of the firing time. In this paper we propose a novel approach based upon Girsanov's Theorem which opens upon new possibilities for answering this question. Analytical approaches of this type are a useful - and wherever possible essential - supplement to computer simulation results, since analytically derived expressions are usually very general, not just for the specific parameter values used in the case of simulation results. We illustrate this by deriving an algebraic form for the interspike interval distribution tail. This could be important for fitting to experimental data, and hence obtaining parameter estimates, but also has implications explored in our previous work (Feng & Brown, 1998a) when the output of the current layer of neurones is the input to a subsequent layer.

When the correlation coefficient between neurones is a constant, we can easily decompose them into a linear summation of independent Poisson processes and therefore all results in the literature are applicable. Under a sufficient condition, we also study the possibility of decomposing a correlated Poisson process into independent Poisson processes. The results can be widely used in biophysical models and experiments.

Finally we discuss the implication of random inputs, i.e. Poisson process inputs, in our model. This is a puzzling issue and a solid answer can be provided only in terms of experiments (Abeles, 1982; Abeles, 1990) . In Mainen & Sejnowski (1995) the authors pointed out that 'Reliability of spike timing depended on stimulus transients. Flat stimuli led to imprecise spike trains, whereas stimuli with transients resembling synaptic activity produced spike trains with timing reproducible to less than one millisecond.' However, it must be emphasised that their experiments were carried out in neocortical *slices*. It is interesting to see that the variability of spike trains depends on the nature of inputs, but CV of efferent spike trains *in vivo* might be very different from those in slices due to the absence of other inputs in slice experiments. For example it has been reported that CV is between 0.5 and 1 for visual cortex (V1) and extrastriate cortex (MT) (Softky & Koch, 1993; Marsalek et al., 1997) even in human motor cells CV is between 0.1 and 0.25 (Matthews (1996) at page 597). There are also examples which demonstrate a group of cells *in vivo* behaving totally differently from in slices. Oxytocin cells fire synchronously *in vivo*, but this property is totally lost in slices (see Brown & Moos, 1997 and references therein). Very recently, it has been reported that random noise of similar amplitude to the deterministic component of the signal plays a key role in neural control of eye and arm movements (Harris & Wolpert, 1998; Sejnowski, 1998). Thus randomness is present - and appears to have a

functionally important role - in a number of physiological functions.

Acknowledgement. We are grateful to the anonymous referees for bringing references (Stevens & Zador, 1998; Gawne & Richmond, 1993) to our attention and their valuable comments on the manuscript. The work was partially supported by BBSRC and an ESEP grant of the Royal Society.

References

Abeles M.(1982). *Local Cortical Circuits: An Electrophysiological Study*, Springer-Verlag: New York.

Abeles M. (1990). *Corticonics*, Cambridge Univ. press: Cambridge, UK.

Abbott L.F., Varela J.A., Sen K., and Nelson S.B.(1997). Synaptic depression and cortical gain control, *Science* **275**, 220-223.

Brown D., and Moos F.(1997). Onset of bursting in oxytocin cells in suckled rats. *J. of Physiology* **503**, 652-634.

Brown D., and Feng J. (1999) Is there a problem matching model and real CV(ISI)? *Neurocomputing* (in press).

Feng, J.(1997), Behaviours of spike output jitter in the integrate-and-fire model. *Phys. Rev. Lett.* **79** 4505-4508.

Feng, J. (1999). Origin Of Firing Varibility Of The Integrate-and-fire Model *Neurocomputing* (in press).

Feng J., and Brown D.(1998a). Spike output jitter, mean firing time and coefficient of variation, *J. of Phys. A: Math. Gen.*, **31** 1239-1252.

Feng J, and Brown D. (1998b). Impact of temporal variation and the balance between excitation and inhibition on the output of the perfect integrate-and-fire model *Biol. Cybern.* **78** 369-376.

Feng J., and Brown D.(1999a). Coefficient Of Variation Greater Than .5 How And When? *Biol. Cybern.* (in press).

Feng J., and Brown D.(1999b). Synchronisation Due To Common Pulsed Input In Stein's Model , (submitted).

Feng, J., Lei, G., and Qian, M. (1992). Second-order algorithms for SDE. *Journal of Computational Mathematics* **10**: 376-387.

Gawne T.J., and Richmond B.J.(1993). How independent are the messages carried by adjacent inferior temporal cortical neurons? *Jour. Neurosci.* **13** 2758-2771.

Harris C.M., and Wolpert D.M.(1998). signal-dependent noise determines motor planning. *Nature* **394** 780-784.

Konig P., Engel A.K., Singer W. (1996) Integrator or coincidence detector? The role of the cortical neuron revisited. *TINS*,**19**, 130-137.

Marsalek P., Koch C., and Maunsell J.(1997). On the relationship between synaptic input and spike output jitter in individual neurones, *Proceedings of the National Academy of Sciences U.S.A.* **94** 735-740.

Matthews P.B.C. (1996). Relationship of firing intervals of human motor units to the trajectory of post-spike after-hyperpolarization and synaptic noise. *J. of physiology* **492**, 597-628.

Mainen Z.F., and Sejnowski, T. J.(1995). Reliability of spike timing in neocortical neurones, *Science* **268**, 1503-1506.

Musila M., and Lánský P.(1994). On the interspike intervals calculated from diffusion approximations for Stein's neuronal model with reversal potentials, *J. Theor. Biol.* **171**, 225-232.

Protter, P. (1980). *Stochastic Integration and Differential Equations. A New Approach.* Berlin: Springer-Verlag.

Ricciardi, L.M., and Sato, S.(1990), Diffusion process and first-passage-times problems. *Lectures in Applied Mathematics and Informatics* ed. Ricciardi, L.M., Manchester: Manchester University Press.

Sejnowski T. J. (1995). Time for a new neural code?, *Nature*, **323** 21-22.

Sejnowski T. J. (1998). Neurobiology - making smooth moves, *Nature*, **394** 725-726.

Sheth B.R., Sharma J., Rao S.C., and Sur M.(1996), Orientataion maps of subjective contours in visual cortex. *Science* **274** 2110-2115.

Softky W., and Koch C.(1993). The highly irregular firing of cortical-cells is inconsistent with temporal integration of random EPSPs, *J. Neurosci.* **13** 334-350.

Shadlen M.N., and Newsome W.T.(1994). Noise, neural codes and cortical organization, *Curr. Opin. Neurobiol.* **4**, 569-579.

Stevens C.F., and Zador A.M.(1998) Input synchrony and the irregular firing of cortical neurons. *Nature Neurosci.* **1** 210-217.

Thomson, A. M.(1997), Activity-dependent properties of synaptic transmission at two classes of connections made by rat neocortical pyramidal, *Jour. of Physiology* **502**, 131-147.

Troyer T.W., and Miller K.D.(1997). Physiological gain leads to high ISI variability in a simple model of a cortical regular spiking cell, *Neural Computation* **9**, 733-745.

Tuckwell H. C. (1988), *Stochastic Processes in the Neurosciences.* Society for industrial and applied mathematics: Philadelphia, Pennsylvania.

Wilbur W.J., and Rinzel J. (1983), A theoretical basis for large coefficient of variation and bimodality in neuronal interspike interval distributions. *J. theor. Biol.* **105** 345-368.

Zohary, E., Shadlen M.N., and Newsome W.T.(1994), Correlated neuronal discharge rate and its implications for psychophysical performance. *Nature* **370** 140-143.

7 Appendix

First of all we know that, in terms of the reflective principle, the distribution density of the first passage time from $(-\infty, V_{thre})$ of a Brownian motion σB_t is given by

$$p(t) = \frac{1}{\sqrt{2\pi t^3 \sigma^2}} V_{thre} \exp(-V_{thre}^2/(2\sigma^2 t))$$

We intend to find the distribution density of the process

$$X_t = \mu t + \sigma B_t$$

For any measureable positive function g we have

$$\langle g(T)) \rangle = \langle \langle g(t) F(t) | \mathcal{F}(\hat{T}) \rangle \rangle \tag{7.1}$$

where $F(t)$ is the Radon-Nikodyn derivative given by the Girsanov's theorem as follows

$$\begin{aligned} F(t) &= \exp(\int_0^t \mu/\sigma dB_s - \frac{1}{2\sigma^2}\int_0^t \sigma^2 ds) \\ &= \exp(\mu/\sigma B_t - \mu^2 t/(2\sigma^2)) \end{aligned}$$

and $\hat{T}$ is the first passage time of B_t. Inserting the expression of $F(t)$ into eq. (7.1) and using the fact that $B_{\hat{T}} = V_{thre}/\sigma$, we obtain

$$\begin{aligned} \langle g(T)) \rangle &= \langle g(\hat{T}) \exp(\mu/\sigma B_{\hat{T}} - \mu^2 \hat{T}/(2\sigma^2)) \rangle \\ &= \int_0^\infty g(t) \exp(\mu V_{thre}/\sigma^2 - \mu^2 t/(2\sigma^2)) \cdot \frac{1}{\sqrt{2\pi t^3 \sigma^2}} V_{thre} \exp(-V_{thre}^2/(2\sigma^2 t)) dt \\ &= \int_0^\infty g(t) \frac{V_{thre}}{\sqrt{2\pi\sigma^2 t^3}} \exp(\mu V_{thre}/\sigma^2 - \mu^2 t/(2\sigma^2) - V_{thre}^2/(2\sigma^2 t)) dt \\ &= \int_0^\infty g(t) \frac{V_{thre}}{\sqrt{2\pi\sigma^2 t^3}} \exp(-(\mu t - V_{thre})^2/(2\sigma^2 t)) dt \end{aligned}$$

Therefore the distribution density of T, the first exiting time of X_t is given by

$$\frac{V_{thre}}{\sqrt{2\pi\sigma^2 t^3}} \exp[-(\mu t - V_{thre})^2/(2\sigma^2 t)]$$